The application of molecular dynamics to fitting EXAFS data

Stephen W.T. Price[1*], Nicholas Zonias[1], Chris-Kriton Skylaris[1], Andrea E. Russell[1*]& Bruce Ravel[2*]

[1] Chemistry, University of Southampton, Highfield, Southampton, SO17 1BJ, UK

[2] National Institute of Standards and Technology, 100 Bureau Drive MS 8520, Gaithersburg MD 20899, USA

Email: s.w.t.price@soton.ac.uk; a.e.russell@soton.ac.uk; bravel@bnl.gov

Abstract. In recent work, a new method for using the outputs of molecular dynamics simulations to generate enhanced inputs for EXAFS analysis of nanoparticles was reported. Although currently limited to the first coordination shell, the method was demonstrated to improve both the quality of the fit, and the cross-correlation of the EXAFS data with that from TEM and XRD. Here we discuss further the justifications behind this assertion.

1. Introduction

Measuring the coordination number of highly disordered systems using EXAFS can be a complex task. When cross-correlating the data with XRD and TEM, the average size determined by EXAFS is smaller [1-3], most often a result of the failure of the fitting model to accurately account for the high degree of disorder present. One of the most common approaches to analysing EXAFS involves quantifying the atom-atom pair distribution, or radial distribution function (RDF), extracted from the data by approximating a Gaussian or near-Gaussian distribution, allowing for the determination of an average coordination number relative to the position of the absorber to be determined, along with the disorder of the absorbing atoms at that distance to be measured. Previously, the addition of higher order cumulants [4] to the analysis has been used to account for small deviations from a Gaussian distribution of bond lengths, whether through skewedness or kurtosis of the distribution. This is effective for small degrees of disorder, however variations on bond length within a sample can give rise to a distribution that is highlynon-Gaussian and therefore cannot be modelled using the cumulant method. Much theoretical work has been reported on the accurate determination of coordination number from EXAFS [5-8]however this has not been directly applied to fitting real data. In these studies the assumption was still on a Gaussian distribution of bond lengths for each coordination shell, with no account for uneven bond length contraction such as that brought about at the surface of a nanoparticle due to termination of the structure.

The effect of surface disorder on the RDF of nanoparticles has recently been investigated by Frenkel [9] and highlights how the increased bond length contraction present at the surface results in a deviation from a Gaussian bond length distribution. This contraction in surface bond length has been observed in coherent diffraction studies of nanoparticles [10]. In recent work we illustrated how the output of a molecular dynamics simulation could be used to provide an enhanced structural input for EXAFS fitting [11]. The nanoparticle structure was simulated [12] using DL_POLY 2.0; the histograms generated from the output and scattering paths generated using Artemis [13]. Full details

of the nanoparticle simulations and characterisation have been published previously [11]. Briefly, four approximately spherical Pt nanoparticles consisting of 55, 177, 381 and 767 atoms, representing sizes of 1.39, 1.94, 2.50 and 3.05 nm respectively were simulated, and the outputs used to generate the histograms that provided the EXAFS fitting inputs.

2. Interpretation of the fits using the molecular dynamics input and histogram approach

Computation of the "true" coordination number of a nanoparticle from MD simulations over a range of temperatures has been shown to differ from those determined from the standard EXAFS analysis [1, 14, 15]. The difference between the real and apparent coordination number is exacerbated by both increases in temperature of the measurement and decreases in the size of the particles under investigation.
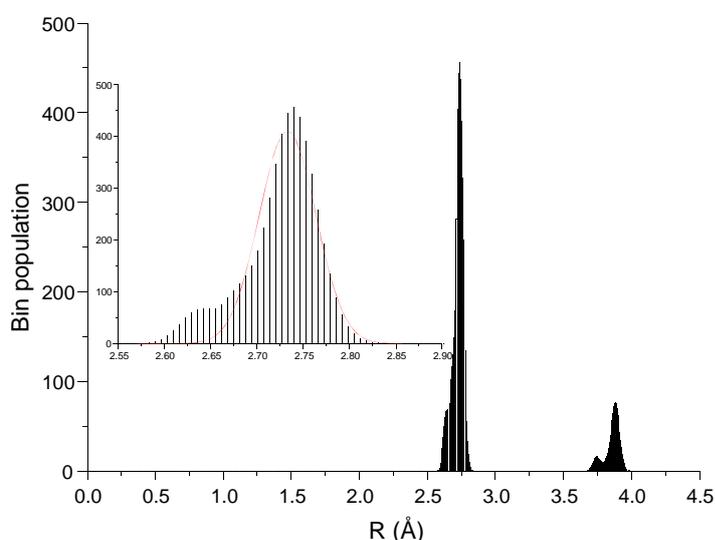
Figure 1: Sample histogram generated from MD output, with Gaussian fit over first shell (red line - inset). Vertical lines are the sum of nearest neighbour bond distances forming a radial distribution function[11].

Table 1: Cross correlation of average particle sizes determined by XRD, TEM and EXAFS analyses (XRD is Rietveld determined average crystallite size). XRD size determination was not possible for the 10 wt.% sample due to very poor crystallinity. The TEM results are volume weighted and the error reported is the standard deviation of the particle size distribution. EXAFS particle size was determined based on the formulae of Jentys [16] and are the average of fits at 20, 150 and 300 K; the reported error is the variance. Results previously published by Price *et al*. [11].

Sample wt.% Pt/C	Average particle size / nm					
	XRD	TEM		EXAFS		
	D_{Vol}	Particles observed	D_{Vol}	Standard	Cumulant	Sutton-Chen
10	---	354	1.6 ± 0.5	1.5 ± 0.1	1.8 ± 0.4	1.6 ± 0.1
20	1.5	445	2.4 ± 0.7	1.9 ± 0.3	2.1 ± 0.4	2.0 ± 0.4
40	1.8	600	2.6 ± 0.7	2.3 ± 0.3	1.9 ± 0.3	2.5 ± 0.3
60	2.3	433	3.0 ± 0.8	2.7 ± 0.3	2.0 ± 0.4	2.9 ± 0.3

For larger nanoparticle systems the contribution of the anharmonicity towards the overall RDF is small as a result of the vast majority of atoms residing in the core of the nanoparticle. In these cases it may be possible for the addition of higher cumulants to adequately model this disorder and therefore provide an improved fit. With smaller nanoparticles, as is the case with those studied here, there is a significant contribution to the RDF from the asymmetry of surface atom contractions (Figure 1) that cannot be adequately described by a Gaussian distribution. As a result the addition of higher cumulants fails to give any physically realistic improvement to the fit. This is most simply observed when comparing the trend in the average particle size (Table 1). The standard EXAFS analysis, XRD and TEM determined particle sizes all follow the same trend with particle loading (as do the results from the MD analysis) however there is no clear trend when adding higher cumulants to the analysis.
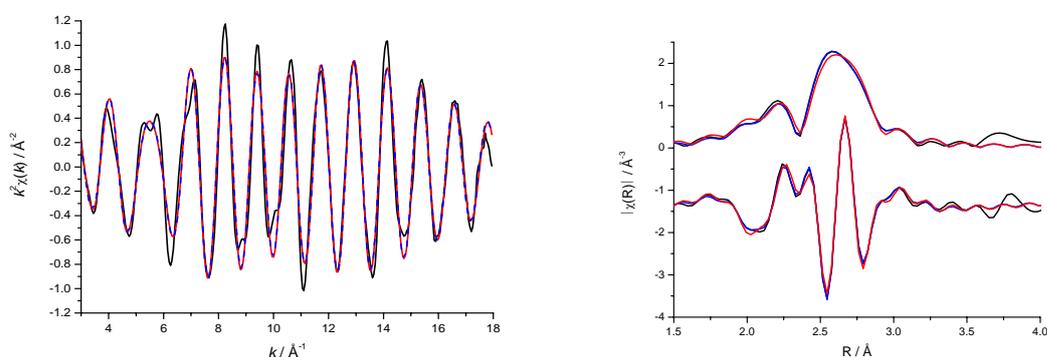
Figure 2: k^2 weighted experimental data (black) and fit to standard model (red), and Sutton-Chen (blue dashed) potentials, along with k^2 weighted magnitude and real Fourier transform for 40 wt.% Pt/C at 150 K[11].
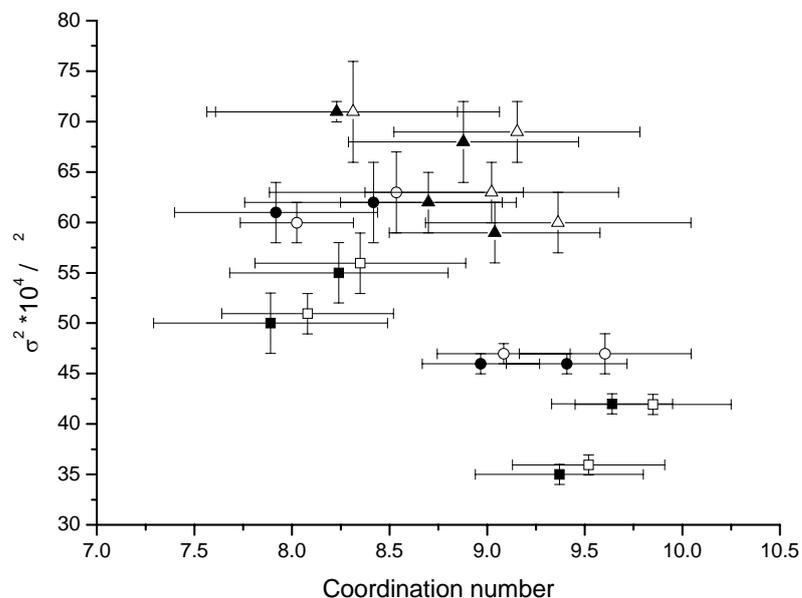
Figure 3: Correlation between coordination number and disorder, σ^2 (sum of σ^2 determined from fit and σ^2 contained in MD output). Closed points are those from the standard method, open points are those from the MD method. The 20 K MD simulations were used as the inputs for the MD approach; experimental data at 20 K is represented by a square marker (□), at 150 K by a circular marker (○) and at 300 K by a triangular marker (Δ).

As previously discussed [11] there is little visual difference in the fits to the data between the standard approach and that using the MD approach, as illustrated in Figure 2. The improvement in the fit of the MD approach over the standard approach is asserted to arise from the reduction of errors for each determined parameter, and the improved goodness of fit. Nominally, a necessary condition for asserting an improved fit is that the parameters differ outside of the error bars. Whilst the coordination numbers and disorder determined from the fits do not necessarily differ outside of the error bars (Figure 3), the trend for each parameter is such that in all cases the average coordination number determined from the fit is larger when using the MD approach. When converted into an average particle size [16] this brings the EXAFS into better correlation with TEM and XRD. The relationship between coordination number and σ^2 in both models and the improvement that the MD approach offers can be better understood by comparing the relationship between the two parameters(Figure 3).

The σ^2 values obtained using the RDF histogram are less than those obtained using the standard model. The disorder of the first shell was calculated directly from the simulation,i.e. the mean square relative displacement of all nearest neighbour atom-atom pair bond lengths, (dotted red arrows, Figure 4) and combined with the σ^2 determined during the fit (red open points, Figure 4) to provide a more direct comparison (open black points Figure 4) with the disorder determined using the standard method (closed black points Figure 4). The smaller nanoparticle simulations contained a higher degree of disorder than the larger simulations. For example, the σ^2 value for the 177 atom simulation (providing the best input to fit the 10 wt.% Pt/C sample – three furthest left open points in Figure 3 and 4) was 0.0016 Å^2 whereas the σ^2 value for the 381 atom simulation (providing the best input to fit all other samples) was only 0.0011 Å^2. Within error, the combined σ^2 values fall in the same range as that determined by the standard method however there is no clear trend; some values are marginally larger, some smaller, and some the same.
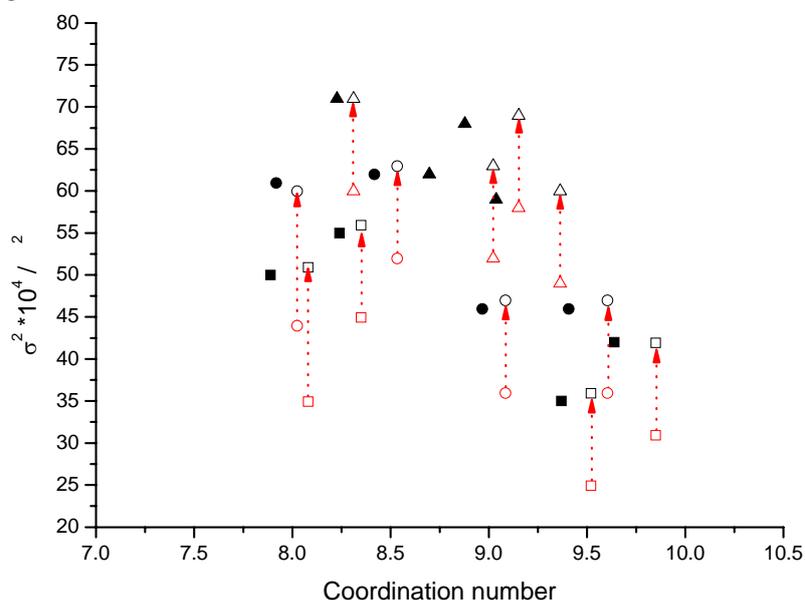
Figure 4: Correlation between coordination number and disorder, σ^2. The black closed points are those determined from the standard fitting approach. The red open points are the values determined from the fit using the histogram without correction. The black open points are the values once the σ^2 computed by the MD has been added to that determined in Demeter. The red arrows are there to link each before and after pair of points. The 20 K MD simulations were used as the inputs for the MD approach; experimental data at 20 K is represented by a square marker (□), at 150 K by a circular marker (○) and at 300 K by a triangular marker (Δ).Error bars are not included for ease of interpretation.

The first shell coordination numbers increase across all of the fits performed resulting in a much clearer trend than with the disorder. Although this is not a large increase in coordination number, and falls within the generally accepted error limits [17] for coordination number determination, the improved qualities of fit indicate that the larger size given by the MD approach is physically reasonable. Indeed when combined with TEM and XRD measurements (Table 1), the MD approach gives a better interpretation of the data than the standard approach and overcomes some of the limitations in applying bulk theory to the analysis of nanoparticles.

Using a more structurally disordered input from the MD gives an improved model to fit the nanoparticles. The MD simulations clearly do not completely model the disorder of the nanoparticle as a σ^2 term is still required in the fit [11, 18]; however it is unlikely that any of the nanoparticles are the perfect "spheres" modelled as is often assumed when fitting nanoparticles.

3. Conclusions

It is worth emphasising that although all of the coordination numbers determined from the fits fall within the error bars, every single time the results consistently shift in the same direction. This shift is as expected, both in light of the cross-correlation with other measurements, and with previous studies of the determination of nanoparticle coordination number [1, 14, 15].For any one individual measurement a comparison of two different fits where the fitted parameters fall within the error bars would hold little to no significance. However, given the same trend occurs for four different samples, measured over a range of temperatures, is independent of the MD simulation used as the input, and that it brings the EXAFS into better agreement with other measurements, we assert that the use of the MD simulations and the histogram approach provides an improved method for fitting nanoparticle EXAFS data. Even with the best experimental set-up there will always be some error associated with the raw data that has an effect on the parameters determined and the quality of fit; however, as the same data set is used to compare each fitting method, this will not be the cause of any differences in the parameters determined from each fitting method. This improved fitting method can also double as a measurable metric for evaluating the effectiveness of molecular dynamics simulations, whether classical or non-classical, for modelling nanoparticle behaviour. Currently, the histogram approach can be applied to single scattering paths generated in Artemis from the molecular dynamics outputs of DL_POLY [12], LAMMPS [19] and VASP [20], with limited effort required to include other sources.

References

[1]   B. S. Clausen, H. Topsøe, L. B. Hansen, P. Stoltze, and J. K. Nørskov 1994, *Catal. Today***21**, 49.

[2]   E. Curis and S. Benazeth 2005, *J. Synchrotron Rad.***12**, 361.

[3]   T. Shido and R. Prins 1998, *J.Phys. Chem. B***102**, 8426.

[4]   G. Bunker 1983, *Nuclear Instruments & Methods***207**, 437.

[5]   R. B. Greegor and F. W. Lytle 1980, *J. Catal.***63**, 476.

[6]   A. I. Frenkel 2007, *Z. Fur Kristallographie***222**, 605.

[7]   J. M. Montejano-Carrizales, F. Aguilera-Granja, and J. L. Moran-Lopez 1997, *NanoStructured Mat.***8**, 269.

[8]   A. M. Beale and B. M. Weckhuysen 2010, *Phys. Chem. Chem. Phys.***12**, 5562.

[9]   A. Yevick and A. I. Frenkel 2010, *Phys. Rev B***81**, 115451.
[10]   W. J. Huang, R. Sun, J. Tao, L. D. Menard, R. G. Nuzzo, and J. M. Zuo 2008, *NatureMat.***7**, 308.
[11]   S. W. T. Price, N. Zonias, C.-K. Skylaris, T. I. Hyde, B. Ravel, and A. E. Russell 2012, *Phys. Rev. B***85**, 075439.
[12]   W. Smith and T. R. Forester 1996, *J. Mol. Graphics***14**, 136 (1996).
[13]   B. Ravel and M. Newville 2005, *J. Synchrotron Rad.***12**, 537.
[14]   B. S. Clausen, H. Topsoe, L. B. Hansen, P. Stoltze, and J. K. Norskov 1993, *Japanese Journal of Applied Physics Part 1-Regular Papers Short Notes & Review Papers***32**, 95.
[15]   B. S. Clausen, L. Grabaek, H. Topsoe, L. B. Hansen, P. Stoltze, J. K. Norskov, and O. H. Nielsen 1993, *J. Catal.***141**, 368.
[16]   A. Jentys 1999, *Phys. Chem. Chem. Phys.***1**, 4059.
[17]   M. Vaarkamp 1998, *Catal. Today***39**, 271.
[18]   O. M. Roscioni, N. Zonias, S. W. T. Price, A. E. Russell, T. Comaschi, and C.-K. Skylaris 2011, *Phys. Rev. B***83**, 115409.
[19]   S. Plimpton 1995, *J. Comp. Phys.***117**, 1.
[20]   G. Kresse and J. Furthmuller 1996*Phys. Rev. B***54**, 11169.